Planetary and Space Science ∎ (∎∎∎∎) ∎∎∎–∎∎∎

Contents lists available at ScienceDirect

Planetary and Space Science

journal homepage: www.elsevier.com/locate/pss

Asteroid orbits with Gaia using random-walk statistical ranging

Karri Muinonen [a,b,*], Grigori Fedorets [a], Hanna Pentikäinen [a], Tuomo Pieniluoma [a], Dagmara Oszkiewicz [c], Mikael Granvik [a,b], Jenni Virtanen [b], Paolo Tanga [d], François Mignard [d], Jérôme Berthier [e], Aldo Dell'Oro [f], Benoit Carry [e], William Thuillot [e]

[a] Department of Physics, Gustaf Hällströmin katu 2a, FI-00014 University of Helsinki, Finland
[b] Finnish Geospatial Research Institute (FGI), Geodeetinrinne 2, FI-02430 Masala, Finland
[c] Institute Astronomical Observatory, Faculty of Physics, Adam Mickiewicz University, ul. Sloneczna 36, PL-60-286 Poznan, Poland
[d] Observatoire de la Côte d'Azur, route de l'Observatoire, BP4229, F-06304 Nice Cedex 4, France
[e] Observatoire de Paris, IMCCE, Institut de mécanique céleste et de calcul des éphémérides, Unité Mixte de Recherche UMR-CNRS 8028, 77 avenue Denfert-Rochereau, F-75014 Paris, France
[f] INAF, Osservatorio Astrofisico di Arcetri, Largo Enrico Fermi 5, I-50125 Firenze, Italy

ARTICLE INFO

Article history:
Received 26 March 2015
Received in revised form
15 October 2015
Accepted 15 October 2015

Keywords:
Asteroids
Near-Earth objects
Orbital inversion
Markov-chain Monte Carlo methods
Random-walk Metropolis–Hastings algorithm
Gaia mission

ABSTRACT

We describe statistical inverse methods for the computation of initial asteroid orbits within the data processing and analysis pipeline of the ESA Gaia space mission. Given small numbers of astrometric observations across short time intervals, we put forward a random-walk ranging method, in which the orbital-element phase space is uniformly sampled, up to a limiting χ^2-value, with the help of the Markov-chain Monte Carlo technique (MCMC). The sample orbits obtain weights from the a posteriori probability density value and the MCMC rejection rate. For the first time, we apply the method to Gaia astrometry of asteroids. The results are nominal in that the method provides realistic estimates for the orbital uncertainties and meets the efficiency requirements for the daily, short-term processing of unknown objects.

1. Introduction

Gaia is an ongoing astrometric mission of the European Space Agency (ESA) with a ground-breaking impact expected on numerous branches of astronomy, including asteroid science (Tanga et al., 2015; Mignard et al., 2007). Unprecedentedly accurate ephemerides for hundreds of thousands of known asteroids, along with the anticipated discovery of asteroids, will be complemented by significantly expanding knowledge of asteroid shapes, sizes, and masses as well as taxonomic classification. Launched in December 2013, Gaia is as of August 2015 routinely observing moving objects, that is, asteroids and other Solar System objects, within a limiting magnitude of $G=20.7$ mag.

In the study of asteroids, orbits are computed from the very moment of discovery onwards. The initial orbits are typically based on small numbers of observations spanning short time intervals. Furthermore, the orbital-longitude intervals covered are minute as compared to the full orbital revolution about the Sun. The Gaia Solar System object short-term processing chain (SSO-ST) has required a robust and efficient method for initial asteroid orbital inversion, enabling the subsequent ground-based follow-up observations of interesting objects. In order to meet this primary requirement, a novel statistical random-walk ranging method is presented in this work, with roots in the earlier ranging methods by Virtanen et al. (2001), Muinonen et al. (2001), and Oszkiewicz et al. (2009).

Several other initial orbit computation methods have been developed by others: for example, Goldader and Alcock (2003) have developed a method targeted for short-arc transneptunian objects. Analogous methods have also been developed for systems of multiple objects: for example, Hestroffer et al. (2005) have introduced a Monte Carlo sampling version of the Thiele-Innes method for binary asteroids. Grundy et al. (2008) have devised a ranging method for transneptunian binaries.

For man-made objects in geocentric orbits, the initial orbit computation problem has been recently addressed by several researchers, in particular, for the linkage problem acute for maintaining space-object catalogues (see, e.g., Siminski et al., 2014

* Corresponding author at: Department of Physics, Gustaf Hällströmin katu 2a, FI-00014 University of Helsinki, Finland. Fax: +358 2941 50610.
E-mail address: karri.muinonen@helsinki.fi (K. Muinonen).

http://dx.doi.org/10.1016/j.pss.2015.10.010
0032-0633/

and references therein). Many of the approaches (Schumacher et al., 2013; DeMars et al., 2012; Fujimoto et al., 2013) use the concept of the admissible region (e.g., Milani et al., 2004), where the range and range-rate space is typically discretized by systematic sampling. Strictly, the approaches can be limited by the linear approximation for the remaining four dimensions. However, when the linear approximation is valid, the systematic ranging method by Farnocchia et al. (2015) (see also Chesley et al., 2005) offers a complete Bayesian treatment of the inverse problem. They introduce an informative a priori probability density for the range and range rate. A full statistical treatment for geosynchronous objects has been put forward by Schneider (2012), who describes an MCMC ranging method using streak-like observations.

The original statistical ranging method (Virtanen et al., 2001; Muinonen et al., 2001) was set out to resolve the long-lasting challenges in the initial computation of orbits. The ranging method starts from the selection of a pair of astrometric observations. Thereafter, the topocentric ranges as well as the angular deviations in Right Ascension (R.A.) and Declination (Decl.) are randomly sampled. The two Cartesian positions allow for the computation of orbital elements and, subsequently, the computation of ephemerides for the observation dates. Candidate orbital elements are included in the sample of accepted elements if the χ^2-value between the observed and computed observations is within a predefined threshold. The sample orbital elements obtain weights based on a meticulous debiasing procedure. When the weights are available, the full sample of orbital elements allows probabilistic assessments for, e.g., object classification, ephemeris computation (cf., Granvik and Muinonen, 2008), as well as the computation of collision probabilities (Virtanen and Muinonen, 2006; Oszkiewicz et al., 2012).

The MCMC ranging method (Oszkiewicz et al., 2009; see also Granvik et al., 2009 and Muinonen et al., 2012) replaces the aforedescribed original sampling algorithm with a proposal probability density function (p.d.f.), and a chain of sample orbital elements results in the phase space. MCMC ranging is based on a bivariate Gaussian proposal p.d.f. for the topocentric ranges, and allows for the sampling to focus on the phase-space domain with most of the probability mass.

In what follows, we carry out statistical ranging of asteroid orbits with the help of random-walk MCMC to map the phase-space regime of acceptable orbital elements. Our novel method is termed random-walk ranging. We apply the methods to example Solar System objects observed by the Gaia mission, highlighting the utilization of the methods in the Gaia data processing and analysis pipeline.

2. Asteroid orbital inversion

2.1. Orbital-element probability density

We describe the six osculating orbital elements of an asteroid at a given epoch t_0 by the vector $\boldsymbol{P}$. For Keplerian orbital elements, $\boldsymbol{P}=(a,e,i,\Omega,\omega,M_0)^T$ (T is transpose) and the elements are, respectively, the semimajor axis, eccentricity, inclination, longitude of ascending node, argument of perihelion, and the mean anomaly at t_0. The angular elements i, Ω, and ω are referred to the ecliptic at equinox J2000.0. For Cartesian elements, $\boldsymbol{P}=(X,Y,Z,\dot{X},\dot{Y},\dot{Z})^T$, where, in a given reference frame at t_0, the vectors $(X,Y,Z)^T$ and $(\dot{X},\dot{Y},\dot{Z})^T$ denote the position and velocity, respectively.

Let $p_{\rm p}$ be the orbital-element probability density function (p.d.f.). Within the Bayesian framework, $p_{\rm p}$ is proportional to the a priori and observational error p.d.f.s $p_{\rm pr}$ and p_ϵ, the latter being evaluated for the sky-plane ("Observed-Computed") residuals $\Delta\boldsymbol{\psi}(\boldsymbol{P})$ (Muinonen and Bowell, 1993):

$$p_{\rm p}(\boldsymbol{P}) \propto p_{\rm pr}(\boldsymbol{P})p_\epsilon(\Delta\boldsymbol{\psi}(\boldsymbol{P})),$$
$$\Delta\boldsymbol{\psi}(\boldsymbol{P}) = \boldsymbol{\psi} - \boldsymbol{\Psi}(\boldsymbol{P}), \tag{1}$$

where $\boldsymbol{\psi}$ and $\boldsymbol{\Psi}$ denote the observations and the computed positions. p_ϵ is typically assumed to be Gaussian.

In order for $p_{\rm p}$ to be invariant in transformations from one set of orbital elements to another, we can regularize the statistical analysis by Jeffreys' a priori p.d.f. (Jeffreys, 1946; cf. Muinonen et al., 2001):

$$p_{\rm pr}(\boldsymbol{P}) \propto \sqrt{\det \Sigma^{-1}(\boldsymbol{P})},$$
$$\Sigma^{-1}(\boldsymbol{P}) = \Phi(\boldsymbol{P})^T \Lambda^{-1} \Phi(\boldsymbol{P}), \tag{2}$$

where Σ^{-1} is the inverse covariance matrix evaluated for the orbital elements $\boldsymbol{P}$, Λ is the covariance matrix for the observational errors and Φ contains the partial derivatives of right ascension and declination with respect to the orbital elements. By the choice of Eq. (2), the transformation of p.d.f.s becomes analogous to that of Gaussian p.d.f.s. The a posteriori orbital-element p.d.f. is then, with the help of the χ^2 value evaluated for the elements $\boldsymbol{P}$:

$$p_{\rm p}(\boldsymbol{P}) \propto \sqrt{\det \Sigma^{-1}(\boldsymbol{P})}\, \exp\left[-\frac{1}{2}\chi^2(\boldsymbol{P})\right],$$
$$\chi^2(\boldsymbol{P}) = \Delta\boldsymbol{\psi}^T(\boldsymbol{P}) \Lambda^{-1} \Delta\boldsymbol{\psi}(\boldsymbol{P}). \tag{3}$$

Securing the invariance in orbital-element transformations makes, e.g., the computation of ephemeris uncertainties and collision probabilities independent of the choice of the orbital-element set (Virtanen and Muinonen, 2006).

As in Oszkiewicz et al. (2009) and Muinonen et al. (2012), Jeffreys' a priori p.d.f. is here replaced by a constant a priori p.d.f. for the Cartesian orbital elements. Strictly, this choice introduces Jacobians when transformed into other orbital elements (e.g., the Keplerian elements). The present approach is supported: first, by the non-singularity of the Cartesian elements underscoring their regularity; second, by the strive for simplicity in the statistical analysis; and, third, by the fact that Jeffreys' a priori p.d.f. is not the only a priori p.d.f. conserving the forms of the a posteriori p.d.f.'s. In summary, with $\boldsymbol{P}=(X,Y,Z,\dot{X},\dot{Y},\dot{Z})^T$, the final a posteriori p.d.f. is

$$p_{\rm p}(\boldsymbol{P}) \propto \exp\left[-\frac{1}{2}\chi^2(\boldsymbol{P})\right],$$
$$\chi^2(\boldsymbol{P}) = \Delta\boldsymbol{\psi}^T(\boldsymbol{P}) \Lambda^{-1} \Delta\boldsymbol{\psi}(\boldsymbol{P}). \tag{4}$$

2.2. Markov-chain Monte Carlo ranging

MCMC methods provide the practical means for sampling complicated, unnormalized p.d.f.s (O'Hagan and Forster, 2004). The Metropolis–Hastings algorithm, utilized presently, is based on the computation of the ratio a_r:

$$a_r = \frac{p_{\rm p}(\boldsymbol{P}')p_{\rm t}(\boldsymbol{P}_j;\boldsymbol{P}')}{p_{\rm p}(\boldsymbol{P}_j)p_{\rm t}(\boldsymbol{P}';\boldsymbol{P}_j)}. \tag{5}$$

Here $\boldsymbol{P}_j$ and $\boldsymbol{P}'$ denote the current and proposed orbital elements in a Markov chain, respectively, and $p_{\rm t}(\boldsymbol{P}';\boldsymbol{P}_j)$ is the proposal p.d.f. from $\boldsymbol{P}_j$ to $\boldsymbol{P}'$ (t stands for transition). The proposed elements $\boldsymbol{P}'$ are accepted or rejected with the help of a uniform random deviate $y \in]0,1[$:

$$\boldsymbol{P}_{j+1} = \begin{cases} \boldsymbol{P}', & y \le a_r, \\ \boldsymbol{P}_j, & y > a_r, \end{cases} \tag{6}$$

that is, the proposed elements are accepted with the probability of $\min(1,a_r)$. After a number of transitions in the so-called burn-in phase, the Markov chain, in the case of success, converges to sample the target p.d.f. $p_{\rm p}$. For monitoring the convergence, there

Please cite this article as: Muinonen, K., et al., Asteroid orbits with Gaia using random-walk statistical ranging. Planetary and Space Science (2015), http://dx.doi.org/10.1016/j.pss.2015.10.010

are various diagnostic tools available (see, e.g., Oszkiewicz et al., 2012).

MCMC ranging (Oszkiewicz et al., 2009) is initiated with the selection of two observations from the full set of observations: typically, the first and the last observation are selected, denoted by A and B. Orbital-element sampling is then carried out with the help of the corresponding topocentric ranges (ρ_A, ρ_B), R.A.s (α_A, α_B), and Decl.s (δ_A, δ_B). These two spherical positions, by accounting for the light time, give the Cartesian positions of the object at two ephemeris dates. The two Cartesian positions correspond to a single, unambiguous orbit passing through the positions at the given dates.

In what follows, we describe how the proposals $\mathbf{Q}' = (\rho'_A, \alpha'_A, \delta'_A, \rho'_B, \alpha'_B, \delta'_B)^T$ for the spherical positions can be obtained. Independent one-dimensional Gaussian proposal p.d.f.s are utilized for transitions in α_A, δ_A, α_B, and δ_B with standard deviations $\sigma_{R.A.}$ and $\sigma_{Decl.}$ (accounting for the cos δ_A and cos δ_B divisors for α_A and α_B, respectively). For ρ_A and ρ_B, a combination of two one-dimensional Gaussian proposal p.d.f.s is used: the topocentric distances are

$$\rho'_A = \rho_{A,j} + y_l + y_r,$$
$$\rho_B{}' = \rho_{B,j} + y_l - y_r, \tag{7}$$

where y_l and y_r are Gaussian random deviates (with standard deviations $\sigma_{\rho,l}$ and $\sigma_{\rho,r}$, respectively) parallel and perpendicular to the line defined by $\rho_A = \rho_B$ in the ρ_A, ρ_B plane. Equivalently, a bivariate Gaussian p.d.f. can be utilized with equal standard deviations σ_ρ and a high positive correlation coefficient $\mathrm{Cor}(\rho_A, \rho_B)$ for ρ_A and ρ_B:

$$\sigma^2_{\rho,l} = \sigma^2_\rho(1 + \mathrm{Cor}(\rho_A, \rho_B)),$$
$$\sigma^2_{\rho,r} = \sigma^2_\rho(1 - \mathrm{Cor}(\rho_A, \rho_B)). \tag{8}$$

In summary, a multivariate Gaussian proposal p.d.f. $p_t(\mathbf{Q}'; \mathbf{Q}_j)$ emerges, where the candidate and current sets of positions are $\mathbf{Q}'$ and $\mathbf{Q}_j$, respectively (cf. Oszkiewicz et al., 2009). The ranges ρ_A and ρ_B are typically highly correlated ($\sigma_{\rho,l} \gg \sigma_{\rho,r}$) and $\sigma_{\rho,l}$ and $\sigma_{\rho,r}$ will differ for different types of objects. The values for the proposal standard deviations $\sigma_{R.A.}$ and $\sigma_{Decl.}$ are typically of the order of the observational error (cf. Eqs. (1) and (2)).

In MCMC ranging, as described above, the proposal p.d.f.s are transformed to the space of two topocentric spherical positions. This transformation introduces Jacobians J_j and J' into the computation of a_r:

$$a_r = \frac{p_p(\mathbf{P}')p_t(\mathbf{Q}_j; \mathbf{Q}')J_j}{p_p(\mathbf{P}_j)p_t(\mathbf{Q}'; \mathbf{Q}_j)J'}, \tag{9}$$

where

$$J_j = \left|\frac{\partial \mathbf{Q}_j}{\partial \mathbf{P}_j}\right|, \quad J' = \left|\frac{\partial \mathbf{Q}'}{\partial \mathbf{P}'}\right|. \tag{10}$$

Finally, since the proposal p.d.f.s $p_t(\mathbf{Q}_j; \mathbf{Q}')$ and $p_t(\mathbf{Q}'; \mathbf{Q}_j)$ are symmetric, the ratio a_r simplifies into

$$a_r = \frac{p_p(\mathbf{P}')J_j}{p_p(\mathbf{P}_j)J'}. \tag{11}$$

2.3. Random-walk ranging

Instead of MCMC ranging, it is typically advantageous to sample in the entire phase-space regime below a given $\chi^2(\mathbf{P})$ level, assigning weights on the basis of the a posteriori probability density value and the Jacobians presented above (cf., Virtanen et al., 2001; Muinonen et al., 2001). Define

$$\Delta\chi^2(\mathbf{P}) = \chi^2(\mathbf{P}) - \chi^2(\mathbf{P}_0), \tag{12}$$

where $\mathbf{P}_0$ specifies a reference orbital solution. Notice that, for linear models and Gaussian p.d.f.s, the definition of Eq. (12) yields the well-known result

$$\Delta\chi^2(\mathbf{P}) = (\mathbf{P} - \mathbf{P}_0)^T \Sigma^{-1}(\mathbf{P}_0)(\mathbf{P} - \mathbf{P}_0), \tag{13}$$

where $\mathbf{P}_0$ denotes the least-squares orbital solution.

Here MCMC ranging is modified for random-walk ranging of the phase space within a given $\Delta\chi^2$ level in Eq. (10) as follows. First, assign a constant, nonzero p.d.f. value for the regime of acceptable orbital elements and assign a zero or infinitesimal p.d.f. value outside the regime. MCMC sampling then returns a set of points that, upon convergence to sampling the phase space of acceptable orbital elements, uniformly characterizes the acceptable regime. Second, assign the a posteriori p.d.f. values as the weights for the sample orbital elements. Since the topocentric spherical coordinates are used in the sampling, the weights need to be further divided by the proper Jacobian value.

In detail, in random-walk ranging uniformly sampling the phase space of the orbital elements, the final weight factor for the sample elements $\mathbf{P}_j$ is

$$w_j = \frac{1}{J_j} p_p(\mathbf{P}_j). \tag{14}$$

As in MCMC ranging, the Markov chain can have the same orbital elements repeating themselves.

How does the present random-walk ranging compare to the original statistical ranging method? With the help of the MCMC theory, the original method can be characterized analogously to the present random-walk ranging. Instead of the random walk, the original method can be viewed as incorporating a proposal p.d.f. from MCMC independence sampling, where the transition is independent of the present position of the Markov chain. As the original method concerns uniform sampling in the phase space of the orbital elements and the sampler is of the independence kind, it is unnecessary to repeat the current elements should the next independent trial be unsuccessful. Thus, combining MCMC and importance sampling terminologies, the original method can be characterized as being the independence-sampler ranging method.

2.4. Software for orbital inversion

The random-walk ranging method is implemented as Java software of the orbital-inversion development unit DU456 (within the coordination unit CU4 entitled *Object processing*) which is currently used by the French Space Agency (CNES) as the initial orbit determination tool in the SSO-ST part of the Gaia Data Processing and Analysis Consortium pipeline (DPAC). DU456 precedes the planning and distribution of observation tasks for the Gaia follow-up network in DU459—a world-wide collaboration of observatories committed to performing follow-up observations within 1–2 days from the Gaia observations. The follow-up network projects the sample orbital elements on the sky plane in order to allow for follow-up observations for refining the orbital elements. Before DU456, the SSO-ST tasks entail the management and implementation of SSO processing (DU450), auxiliary data (DU451), identification of known objects (DU452), CCD processing (DU453), astrometric reduction (DU454), and object threading (DU455).

The random-walk ranging method, along with the original and MCMC ranging methods, are implemented in the publicly available Fortran95 asteroid-orbit-computation software package OpenOrb (Granvik et al., 2009). In particular, the DPAC Java and the OpenOrb Fortran95 implementations of the random-walk ranging method have been cross-validated. We endeavour to maintain a collection of state-of-the-art methods for asteroid orbit computation.

Please cite this article as: Muinonen, K., et al., Asteroid orbits with Gaia using random-walk statistical ranging. Planetary and Space Science (2015), http://dx.doi.org/10.1016/j.pss.2015.10.010

3. Results and discussion

We use the astrometric data sets observed by Gaia on November 7–9, 2014 for 89 known asteroids that, in accordance with the Gaia publication rules, must remain anonymous in the present context. The data for each asteroid consist of 2–7 transits. Each transit corresponds to a single sweep of the appropriate sector of the sky. In turn, each transit includes 1–10 separate observations. It follows that the present data sets consist of 2–70 observations.

As most of the objects to be observed are in the main belt of asteroids, the initial guess for the ranges is centered at 2.5 au with $\sigma_\rho = 0.2$ au and $\mathrm{Cor}(\rho_A, \rho_B) = 0.999$. In other words, the ratio $\sigma^2_{\rho,l} : \sigma^2_{\rho,r} \approx 2000 : 1$ (Eq. (8)). The values of R.A. and Decl. are drawn from a Gaussian proposal centered around the first and last observations of the data set with standard deviations of $\sigma_{\mathrm{R.A.}} \approx 10$ mas and $\sigma_{\mathrm{Decl.}} \approx 5$ mas, respectively.

The burn-in phase is replaced by an optimization phase in order for the chain to converge to the regime of acceptable orbits. Transitions are proposed with the aforedescribed Gaussian proposal p.d.f. and accepted only when they result in improved χ^2-values. After four consecutive orbits within the acceptable χ^2-regime, the algorithm switches to random-walk ranging without any specific burn-in phase. If no acceptable solutions are found during the 50 first attempts of the optimization phase, the range proposal is changed to be randomly drawn from values within [1 au, 6 au], whereafter the optimization phase is repeated.

For each observation set, we have produced 2000 ranging solutions with $\chi^2(\boldsymbol{P}) - \chi^2(\boldsymbol{P}_0) < 20.0$, corresponding, approximately, to the $3-\sigma$ confidence regime ($\sim$99.7%). The computations took 6 min 55 s for 89 objects (178,000 orbits altogether) on a standard 4-core laptop computer, including the initial optimization phase. For all but one case, 2000 orbits were generated.

As for the orbital uncertainties, the most important factor is the time interval spanned by the observations. Increasing the interval effectively decreases the phase-space volume of possible solutions, up to the point where the solutions are well constrained to a small volume. The collapse of the orbital uncertainties is also described as being a phase transition (see, e.g., Muinonen et al., 2006).

In what follows, we assess two examples U1 and U2 in detail, U standing here for "unidentified". The examples are chosen, on one hand, based on the variety of the data available, and, on the other hand, retrospectively based on the characteristics of the resulting orbital distributions. For practical purposes of initial orbital inversion, mapping the phase space of possible solutions is more important than obtaining large numbers of sample orbits with significant weights.

The observed objects are most likely to be main-belt objects (MBOs). No near-Earth-object candidates have been found in the data set, and a handful of objects other than MBOs are present. Some of these MBOs have a rather well confined inclination and longitude of the ascending node. Solutions for U1 and U2 are presented in Figs. 1 and 2 as sets of random-walk ranging samples against the semimajor axis with colors denoting the weights.

The main difference in the input data of the two examples is the observational time interval — in the case U1 in Fig. 1, the interval is 1 h 47.3 min, whereas, in the case of U2 in Fig. 2, the interval is 19 h 47.3 min. As can be seen, in the latter case, the Keplerian orbital-element phase-space regime spanned is substantially smaller. Nevertheless, in both cases, markedly differing Keplerian orbital elements are sampled. For example, the a–e plots indicate that orbital longitudes near perihelion as well as near aphelion are capable of matching the observations.

We have extended the analysis of the discovery data by propagating the sample orbits one day forward after the final observation date. We calculated the ephemeris and the standard deviations for the ephemerides of the entire data set. For this part, we used OpenOrb (Granvik et al., 2009) and generated 10,000 orbits for each observation set. The distribution of the

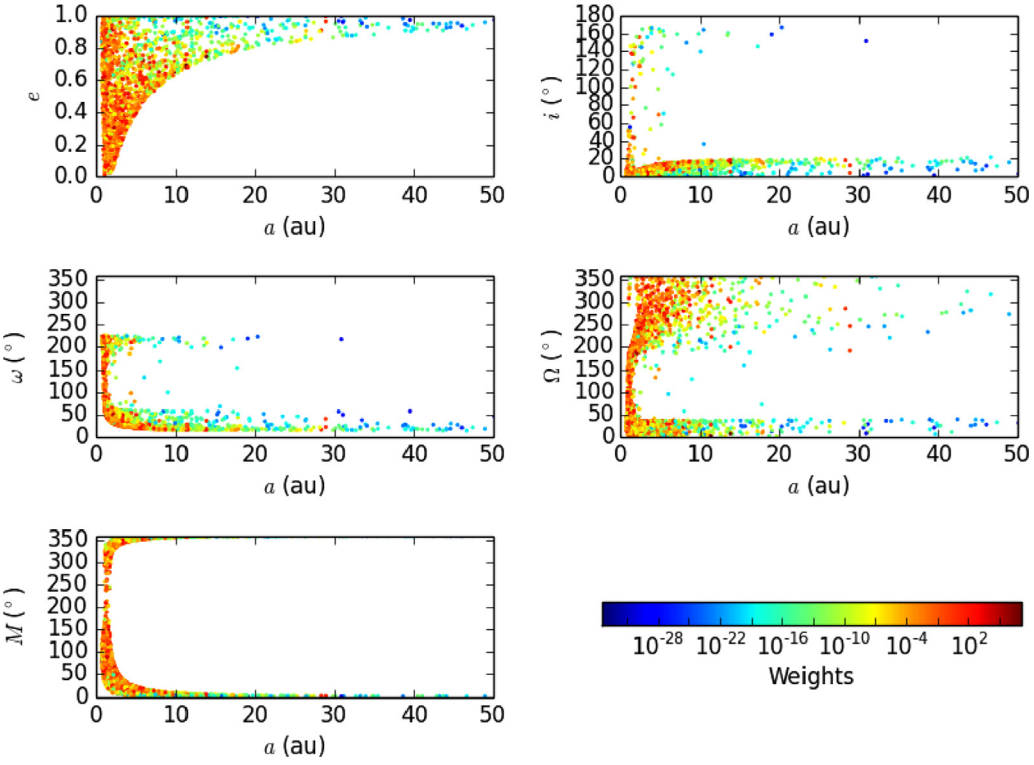

Fig. 1. Keplerian orbital elements from random-walk ranging for the object U1 (see text) with 15 observations from two transits with an observational time interval of less than 2 h, illustrating wide distributions typical for such data sets.

Please cite this article as: Muinonen, K., et al., Asteroid orbits with Gaia using random-walk statistical ranging. Planetary and Space Science (2015), http://dx.doi.org/10.1016/j.pss.2015.10.010

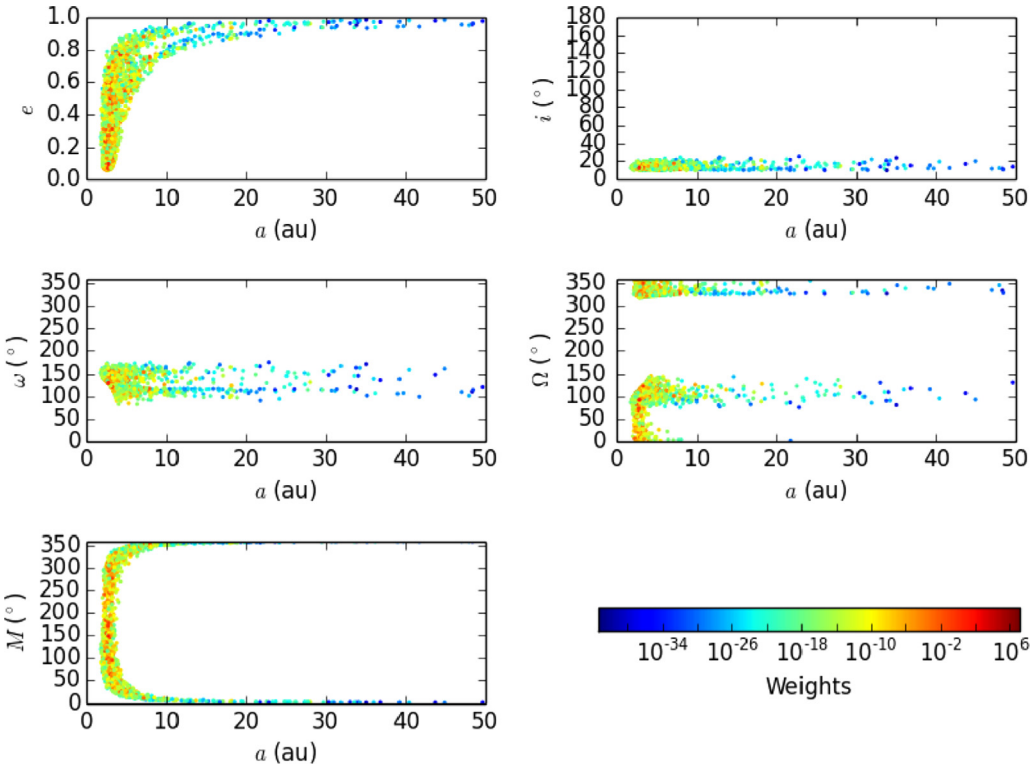

Fig. 2. As in Fig. 1 for the object U2 with 35 observations from seven transits with an observational time interval of almost 20 h, illustrating one of the best available data sets. The asteroid is likely to be a main-belt object, and the weights already indicate a preferred phase-space regime.

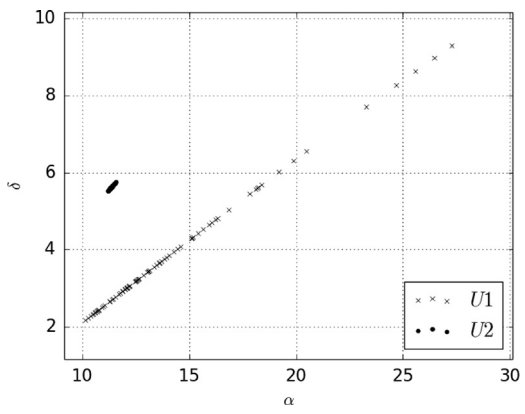

Fig. 3. The geocentric ephemeris prediction in R.A. and Decl. for the objects U1 and U2 using 10^4 orbits propagated to a date 1.0 d after the last Gaia observation date. For U1, the standard deviations for the ephemeris prediction are $\sigma_\alpha = 3.8^\circ$ and $\sigma_\delta = 1.6^\circ$, whereas for the object U2, $\sigma_\alpha = 0.06^\circ$ and $\sigma_\delta = 0.04^\circ$. The ephemerides are shifted for better display.

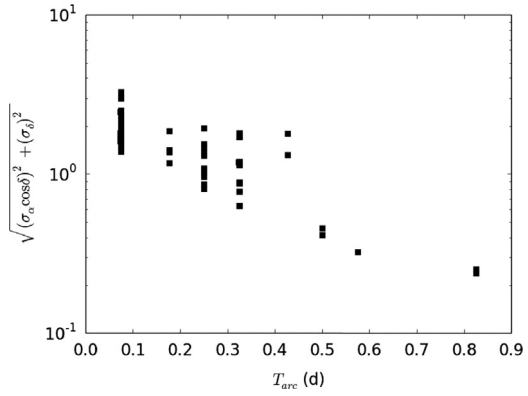

Fig. 4. The standard deviations in R.A. and Decl. combined into $\sqrt{(\sigma_\alpha \cos\delta)^2+(\sigma_\delta)^2}$ for 89 objects using 10^4 orbits propagated 1.0 d forward from the last Gaia observation date as a function of the observational time interval.

ephemerides for the objects with extreme values of observational time intervals are presented in Fig. 3 for objects with minimum (on the left) and maximum time intervals (on the right).

In Fig. 4, we present the total sky-plane uncertainties $\sqrt{\sigma_\alpha^2 \cos^2\delta + \sigma_\delta^2}$ as a function of the observational time interval. The large variety of standard deviations for solutions with short arcs probably owes to the fact that the direction along which the ephemeris predictions are aligned results from the geometry and observational pattern of Gaia, i.e. the observations constrain the orbital solutions along the scanning direction but not as well in the direction perpendicular to the scanning direction. Furthermore, due to the short observational time intervals, the Gaia-centric distances of the objects are poorly constrained.

Although the phase-space volume of solutions is constantly decreasing with time, it is not until the time interval of about 12 h that the volume becomes significantly constrained. However, further data are required to confirm this tentative conclusion. The warning is raised due to the small current number of cases with time intervals exceeding 12 h.

In SSO-ST, the random-walk ranging software is not utilized for asteroid identification: that is carried out before the orbital inversion. However, for a handful of objects in the present data set, objects have been identified in order to facilitate a comparison of ephemerides from the present orbital inversion and from the precise orbits. All but one of the true positions were within the sky-plane uncertainty regimes predicted from the present sample orbits.

For the particular task of the Gaia data-processing pipeline, the parameters set for the random-walk ranging work relatively well. Among 89 different objects, there has been only one for which no

Please cite this article as: Muinonen, K., et al., Asteroid orbits with Gaia using random-walk statistical ranging. Planetary and Space Science (2015), http://dx.doi.org/10.1016/j.pss.2015.10.010

orbital solutions could be obtained and that may have been due to an erroneous data set.

4. Conclusions

We have introduced a novel random-walk ranging method for the initial computation of asteroid orbits. In the method, we characterize the phase-space regime within a pre-defined χ^2-value by using MCMC for the generation of orbital elements. We then assign weights to the elements on the basis of their a posteriori probability-density values accompanied with local Jacobians.

The random-walk ranging method resembles the original and MCMC ranging methods. On one hand, random-walk ranging is insensitive to local extrema in the phase space, efficiently mapping the geometry of the acceptable phase-space regime. This is somewhat contrary to MCMC ranging that can face difficulties with multimodal probability densities. On the other hand, random-walk ranging can suffer from producing a scarce sample of orbital elements with small χ^2-values, as in the original ranging method. The advantages of random-walk ranging over other initial orbit computation methods are its robustness and computational speed.

We have successfully applied random-walk ranging to 89 asteroids observed by Gaia, constituting a validation of the SSO-ST part of the Gaia DPAC pipeline. The produced orbital elements for known objects are in agreement with the orbital elements for these objects computed at the Minor Planet Center. It is notable that the present data are the first Gaia data ever available for orbital inversion with random-walk ranging.

We can anticipate successful asteroid discoveries by Gaia as a result of the follow-up observations based on the orbital elements from random-walk ranging. In the future, we will continue to assess the a priori probability densities in the cases of scarce observational data. Furthermore, we will compare the computational speed of the random-walk ranging method to that of other initial orbital-inversion methods and we will optimize the method for different classes of asteroids.

Acknowledgments

We are grateful to the Gaia Data Processing and Analysis Consortium for providing an impressive Java environment for asteroid orbital inversion. In CU4, Thierry Pauwels and Jean-Marc Petit have managed the development units DU454 and DU455, respectively, responsible for astrometric reduction and object threading. Alberto Cellino and Marco Delbó are acknowledged for constructive comments during the evolution of the DU456 orbital-inversion software. CNES has provided valuable software development support. Research funded, in part, by the Academy of Finland (KM's project 1257966). GF acknowledges the support of the Magnus Ehrnrooth foundation. ADO thankfully acknowledges financial support from the Italian Space Agency (ASI contracts Gaia Mission - The Italian Participation to DPAC, 2014-025-R.0).

References

Chesley, S.R., 2005. Very short arc orbit determination: the case of asteroid 2004 FU162. In: Knežević, Z., Milani, A. (Eds.), Proceedings of IAU Colloquium 197—Dynamics of Populations of Planetary Systems. Cambridge University Press, Cambridge, pp. 255–258.

DeMars, K.J., Jah, M.K., Schumacher Jr., P.W., 2012. Initial orbit determination using short-arc angle and angle rate data. IEEE Trans. Aerosp. Electron. Syst. 48 (3), 2628–2637.

Farnocchia, D., Chesley, S.R., Micheli, M., 2015. Systematic ranging and late warning asteroid impacts. Icarus 258, 18–27.

Fujimoto, K., Scheeres, D.J., Herzog, J., Schildknecht, T., 2013. Association of optical tracklets from a geosynchronous belt survey via the direct Bayesian admissible region approach. Adv. Space Res. 53 (2), 295–308.

Goldader, J.D., Alcock, Ch., 2003. Constraining recovery observations for trans-neptunian objects with poorly known orbits. Publ. Astron. Soc. Pac. 115, 1330–1339.

Granvik, M., Muinonen, K., 2008. Asteroid identification over apparitions. Icarus 198, 130–137.

Granvik, M., Virtanen, J., Oszkiewicz, D., Muinonen, K., 2009. OpenOrb: open-source asteroid-orbit-computation software including ranging. Meteorit. Planet. Sci. 44 (12), 1853–1861.

Grundy, W.M., Noll, K.S., Virtanen, J., Muinonen, K., Kern, S.D., Stephens, D.C., Stansberry, J.A., Levison, H.F., Spencer, J.R., 2008. (42355) Typhon Echidna: scheduling observations for binary orbit determination. Icarus 197, 260–268.

Hestroffer, D., Vachier, F., Balat, B., 2005. Orbit determination of binary asteroids. Earth Moon Planets 97, 245–260.

Jeffreys, H., 1946. An invariant form for the prior probability in estimation problems. Proc. R. Stat. Soc. Lond. Ser. A 186, 453–461.

Mignard, F., Cellino, A., Muinonen, K., Tanga, P., Delbò, M., Dell'Oro, A., Granvik, M., Hestroffer, D., Mouret, S., Thuillot, W., Virtanen, J., 2007. The Gaia mission: expected applications to asteroid science. Earth Moon Planets 101 (3–4), 97–125.

Milani, A., Gronchi, G., Vitturi, M.D.M., Knezevic, Z., 2004. Orbit determination with very short arcs. I admissible regions. Celest. Mech. Dyn. Astron. 90 (1–2), 57–85.

Muinonen, K., Bowell, E., 1993. Asteroid orbit determination using Bayesian probabilities. Icarus 104, 255–279.

Muinonen, K., Virtanen, J., Bowell, E., 2001. Collision probability for Earth-crossing asteroids using orbital ranging. Celest. Mech. Dyn. Astron. 81, 93–101.

Muinonen, K., Virtanen, J., Granvik, M., Laakso, T., 2006. Asteroid orbits using phase-space volumes of variation. Mon. Not. R. Astron. Soc. 368, 809–818.

Muinonen, K., Granvik, M., Oszkiewicz, D., Pieniluoma, T., Pentikäinen, H., 2012. Asteroid orbital inversion using a virtual-observation Markov-chain Monte Carlo method. Planet. Space Sci. 73, 15–20.

O'Hagan, A., Forster, J., 2004. Kendall's Advanced Theory of Statistics, vol. 2B, second edition. Bayesian Inference, Arnold.

Oszkiewicz, D., Muinonen, K., Virtanen, J., Granvik, M., 2009. Asteroid orbital ranging using Markov-chain Monte Carlo. Meteorit. Planet. Sci. 44 (12), 1897–1904.

Oszkiewicz, D., Muinonen, K., Virtanen, J., Granvik, M., Bowell, E., 2012. Modeling collision probability for Earth-impactor 2008 TC_3. Planet. Space Sci. 73 (1), 30–38.

Schneider, M.D., 2012. Bayesian linking of geosynchronous orbital debris tracks as seen by the Large Synoptic Survey Telescope. Adv. Space Res. 49 (4), 655–666.

Schumacher Jr., P.W., Wilkins, M.P., Roscoe, C.W.T., 2013. Parallel algorithm for track initiation for optical space surveillance. In: Proceedings of the Sixth European Conference on Space Debris, Darmstadt, Germany.

Siminski, J.A., Montenbruck, O., Fiedler, H., Schildknecht, T., 2014. Short-arc tracklet association for geostationary objects. Adv. Space Res. 53, 1184–1194.

Tanga, P., Dell'Oro, A., Mignard, F., Muinonen, K., Pauwels, T., Thuillot, W., Berthier, J., Cellino, A., Hestroffer, D., Petit, J.-M., Carry, B., Delbó, M., Fedorets, G., Galluccio, L., Granvik, M., Ordenovic, C., Pentikäinen, H., 2015. The daily processing of asteroid observations by Gaia. Planet. Space Sci., this issue.

Virtanen, J., Muinonen, K., 2006. Time evolution of orbital uncertainties for impactor candidate 2004 AS_1. Icarus 184 (2), 289–301.

Virtanen, J., Muinonen, K., Bowell, E., 2001. Statistical ranging of asteroid orbits. Icarus 154, 412–431.

Please cite this article as: Muinonen, K., et al., Asteroid orbits with Gaia using random-walk statistical ranging. Planetary and Space Science (2015), http://dx.doi.org/10.1016/j.pss.2015.10.010